

22

23

Abstract

24

Objective: Paracondylar (PCP) and epitransverse processes (ETP) represent rare types of articulations that can occur between the occipital bone and the transverse process of atlas vertebra.

25

26

27

28

Material and methods: Five systematic search strings were conducted on PubMed database on 14.01.2022. The search was conducted by one observer to identify studies on PCP, and on ETP in living patients. Open and close access articles were selected as this topic is infrequently described in the main medical literature.

29

30

31

32

33

34

Results: We provided with a pictorial review of 1) Paracondylar tubercle, 2) Unilateral PCP with cylindrical shape, 3) Unilateral PCP with pyramidal shape, 4) Unilateral PCP with lateral joint with transverse process, 5) Unilateral PCP with superior joint and partial fusion with transverse process, 6) Unilateral ETP with neocondyle and joint with occipital condyle, 7) Unilateral ETP with joint with occipital bone, 8) Unilateral ETP with a bony bridge with lateral mass (ponticulus lateralis), and 9) Bilateral variation: paracondylar mass and ETP.

35

36

37

38

39

40

41

42

Conclusions: Six figures were found in the selected literature and belong only to articles published in closed access. We provided with additional 41 open access freely available figures. We were first to present CBCT reference figures of:

43

44

45

46

47

48

49

50

51

52

1) Unilateral paracondylar tubercle, 2) Fusion of PCP with the transverse process of C1, 3) Joint between ETP and the lateral side of occipital condyle, and 4) Presence of bony bridge (ponticulus lateralis) between ETP and the lateral mass of C1. We were also first to describe a bilateral mixt variation with paracondylar mass on one side and ETP on the other side of C1. An open and accessible knowledge support (such as Nemesis journal) is needed to easily find clinical reference CBCT figures of craniocervicofacial bone variations.

53

54

55

Keywords: paracondylar process, epitransverse process, CBCT, variation, chronic headache.

56

57

Introduction

58 Paracondylar (PCP) and epitransverse (ETP) processes were first described by
59 Meckel in 1815 and by Cruveilhier in 1851 as additional articulation of the occipital
60 bone with the transverse process of the atlas [1]. First anatomical description of
61 PCP/ETP was provided by McRae in 1960 [2, 3]. Especially PCP received diverse
62 anatomical names such as paramastoid process [1], paracondylar process [1, 3-5],
63 paraoccipital process [1], parajugular process [1], estiloid process [1], or inferior
64 extension of the jugular process of the occipital bone [1].

65 Fourth occipital sclerotome, or proatlas, contributes to the development of the
66 foramen magnum, of occipital condyles, of atlantal masses, and of the superior
67 portion of the posterior arch of C1 [4]. For McCall et al., PCP results from a
68 disruption of the normal development of the proatlas [4].

69 The shape of PCP is traditionally described as cone-shaped bony exostosis, arising
70 medial to the mastoid process and posterolateral to the occipital condyles, located at
71 the side of the insertion of the musculus rectus capitis lateralis [1, 5]. For De
72 Grauw et al., and Shah et al., PCP is an embryologic derivative of the cranial part of
73 the first cervical or of the last occipital sclerotome [1, 6].

74 The prevalence is 0.077% to 2% in medical reports [3, 4-6], and over 40% in
75 anthropological studies [5]. Larger processes are considered rarer than the minor
76 tubercles, and tend to be unilateral [5, 6]. Small tubercles are often bilateral and
77 are revealed with CT scan or MRI [5].

78 Symptoms arising from PCP/ETP complex could be due to mechanical compression
79 of the nerve structures (C1 root), compression of the vascular structures, instability,
80 and rigidity, or all of them mainly due to a biomechanical alteration of the
81 osteochondral junction [3].

82 Larger processes articulating with or fused with the atlas may produce symptoms
83 such as: uni- [6] or bilateral headache localized in the upper zone of the neck with
84 radiation to the parietal and frontal area [3], occipitocervical pain [4], postural
85 alterations, and limited or blocked neck movements (torticollis) [3, 5]. Headache
86 related with the presence of symptomatic PCP/ETP was described as worsening in
87 the evening [3, 5]. Patients with PCP/ETP variation who suffered from head trauma
88 may present with exaggerating pain (chronic headache attributed to other head
89 and/or neck trauma) and with restricted range of head motion [5]. In case of chronic
90 headache without relieve by conservative therapy, neurosurgical removing the PCP
91 gives improvement of the headache [4, 5].

92 Proposed treatments in the literature were conservative [6, 7], steroid injections [4],
93 and even neurosurgery [4, 6].

94

95 In this article we provide with an updated classification of PCP/ETP types based
96 on 1) systematic search of the literature, and 2) on a series of 9 asymptomatic

97 patients who undergo cone beam computed tomography (CBCT) for other reason.
98 This rare anatomical variation was an incidental finding in all cases.

99 **Materials and methods**

100 Five systematic search strings were conducted on PubMed database on
101 14.01.2022. The search was conducted by one observer to identify studies on PCP,
102 and on ETP in living patients. Open access and close access articles were selected as
103 this topic is infrequently described in the main medical literature. There was no time
104 frame for the search. The selected languages were English, French and Italian. The
105 inclusion criteria were: articles with abstracts, clinical human studies, case reports,
106 case series illustrated with CT scan and/or cone beam CT imaging. The exclusion
107 criteria were articles without abstracts, animal studies, *in vitro* studies, cadaveric
108 studies, studies using dry skulls and/or dry vertebra, forensic studies, other imaging
109 than CT scan and/or cone beam CT. The final selection was performed after reading
110 the full article. In the selected studies we searched for CT scan and/or CBCT
111 iconography for diagnostic of PCP and ETP.
112

113 The first search equation was on “paracondylar process”, and was set as following:
114 "paracondylar"[All Fields] AND ("process"[All Fields] OR "proceso"[All Fields]
115 OR "processed"[All Fields] OR "processes"[All Fields] OR "processing"[All Fields]
116 OR "processings"[All Fields]). The search was performed on 14.01.2022 by one
117 observer.

118 We found 30 articles with 5 articles selected [3-7] and 25 articles excluded.

119

120 The second search equation was on “paramastoid process”, and was set as
121 following: "paramastoid"[All Fields] AND ("process"[All Fields] OR "proceso"[All
122 Fields] OR "processed"[All Fields] OR "processes"[All Fields] OR "processing"[All
123 Fields] OR "processings"[All Fields]). The search was performed on 14.01.2022 by
124 one observer.

125 We found 10 articles, and 10 articles were excluded.

126

127 The third search equation was on “third occipital condyle”, and was set as following:
128 ("third"[All Fields] OR "thirds"[All Fields]) AND ("occipital"[All Fields] OR
129 "occipitally"[All Fields] OR "occipitals"[All Fields]) AND ("bone and
130 bones"[MeSH Terms] OR ("bone"[All Fields] AND "bones"[All Fields]) OR "bone
131 and bones"[All Fields] OR "condyle"[All Fields] OR "condyles"[All Fields] OR
132 "condyl"[All Fields] OR "condyle s"[All Fields]). The search was performed on
133 14.01.2022 by one observer.

134 We found 243 articles, and 243 articles were excluded.

135

136 The fourth search equation was on “accessory occipital condyle”, and was set as
137 following: ("accessories"[All Fields] OR "accessory"[All Fields]) AND

138 ("occipital"[All Fields] OR "occipitally"[All Fields] OR "occipitals"[All Fields])
139 AND ("bone and bones"[MeSH Terms] OR ("bone"[All Fields] AND "bones"[All
140 Fields]) OR "bone and bones"[All Fields] OR "condyle"[All Fields] OR
141 "condyles"[All Fields] OR "condyl"[All Fields] OR "condyle s"[All Fields]).

142 The search was performed on 14.01.2022 by one observer. We found 78 articles,
143 and 78 articles were excluded.

144
145 Th fifth search equation was on “epitransverse process”, and was set as following:
146 "epitransverse"[All Fields] AND ("process"[All Fields] OR "processe"[All Fields]
147 OR "processed"[All Fields] OR "processes"[All Fields] OR "processing"[All Fields]
148 OR "processings"[All Fields]). The search was performed on 14.01.2022 by one
149 observer. We found 9 articles found, and 9 articles were excluded.

150
151 Only the first search string provided 5 articles for the review [3-7]. The four other
152 search strings gave no additional selected articles as found articles fit with exclusion
153 criteria, or were duplicate articles in relation with the first search equation.

154
155 As this variation is rare we searched also for information on the free website of the
156 international foundation Radiopaedia.org
157 (<https://radiopaedia.org/articles/paracondylar-process?lang=us>),
158 (<https://radiopaedia.org/articles/epitransverse-process-of-the-atlas>) and we found
159 one CT scan illustrated case for PCP and one for ETP.

160
161
162
163
164
165
166
167
168
169
170
171
172
173
174
175
176
177
178
179
180
181

182

Results

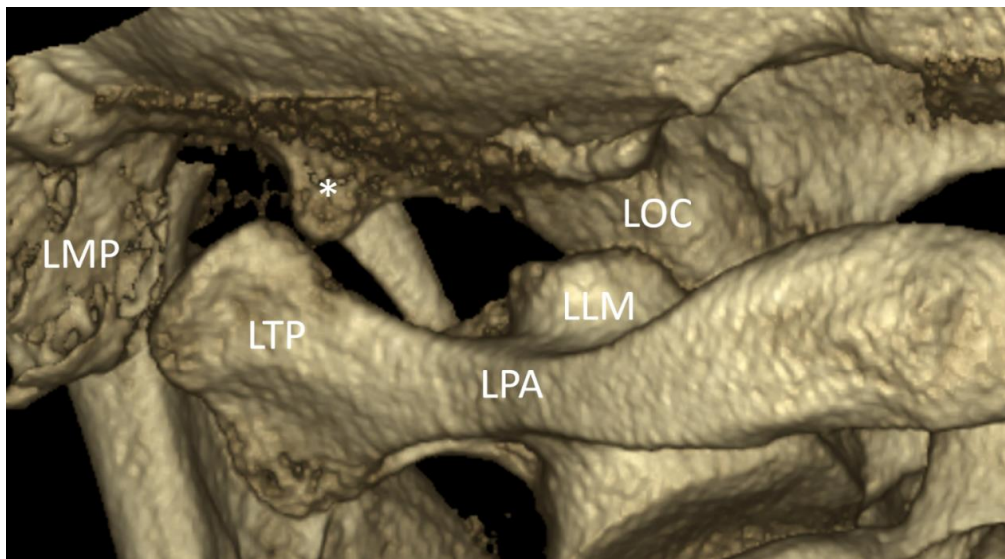
183

In CBCT records from our Department of oral and maxillofacial surgery we found 9 patients presenting with PCP and ETP.

184

185

Paracondylar tubercle



186

Fig. 1. Patient n°1. Planmeca Promax 3D Mid. Three-dimensional (3D) reconstruction. Posterior view of the occipital bone and the atlas vertebra (C1). *Left paracondylar tubercle. LOC: left occipital condyle. LLM: left lateral mass of C1. LPA: left posterior arch of C1. LTP: left transverse process of C1. LMP: left mastoid process. Close relationship between *Left paracondylar tubercle is close to LTP but without the presence of a joint structure.

187

188

189

190

191

192

193

194

195

196

197

198

199

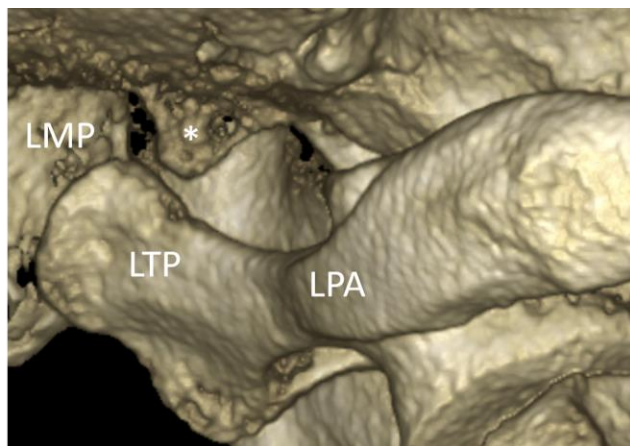
200

201

202

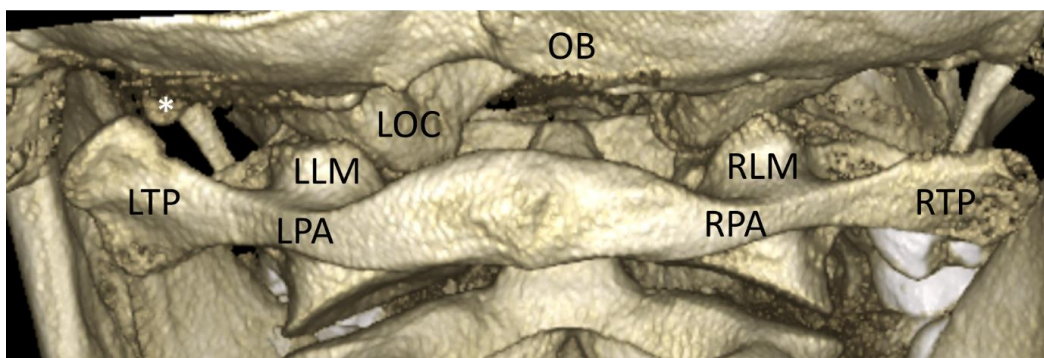
203

204



205
206
207
208
209
210
211

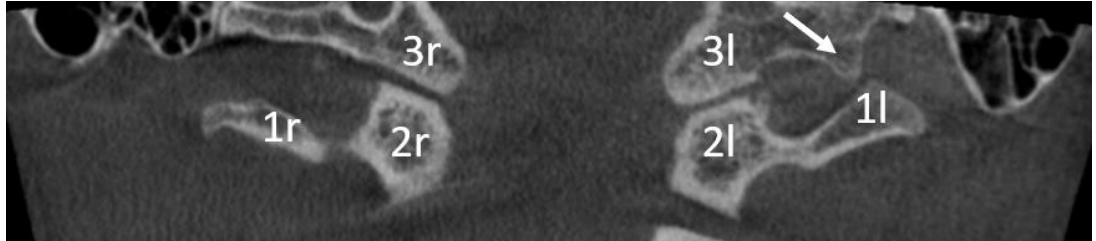
Fig. 2. Patient n°1. Planmeca Promax 3D Mid. 3D reconstruction. Closer posterior and left lateral view. * Left paracondylar tubercle. LPA: left posterior arch of atlas. LTP: left transverse process of C1. LMP: left mastoid process. Close relationship between *Left paracondylar tubercle and LTP without the presence of a joint structure.



212

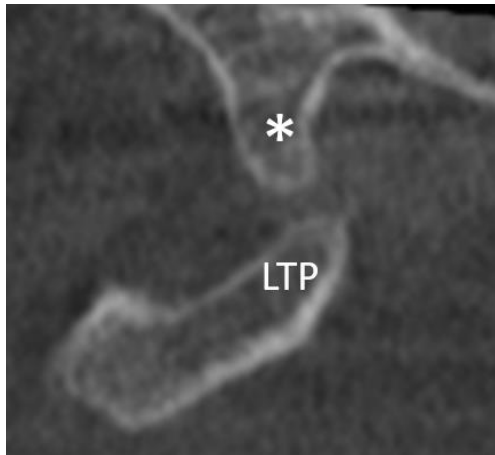
213
214
215
216
217
218
219
220
221
222
223
224

Fig. 3. Patient n°1. Planmeca Promax 3D Mid. 3D reconstruction. Posterior view. *Left paracondylar tubercle. OB: occipital bone. LOC: left occipital condyle. LLM: left lateral mass of C1. RLM: right lateral mass. LPA: left posterior arch. RPA: right posterior arch. LTP: left transverse process. RTP: right transverse process. Difference in shape between left and right transverse process, with the upper edge of the LTP more pyramidal, and the upper edge of RTP flatter.



225
226
227
228
229
230
231
232

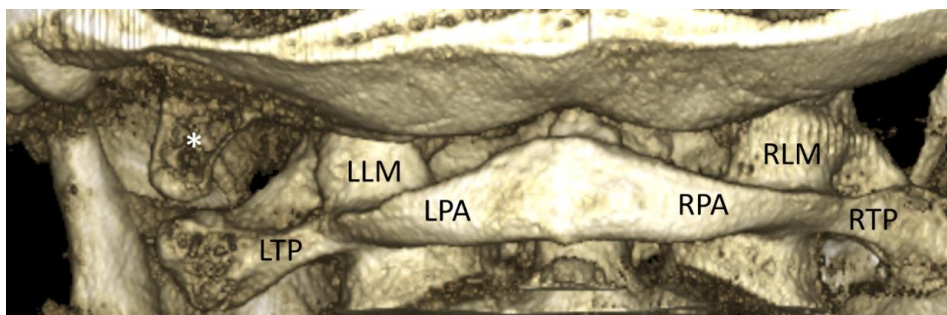
Fig. 4. Patient n°1. Planmeca Promax 3D Mid. Coronal two-dimensional (2D) view. Posterior view of the C1, of the foramen magnum, and of the occipital bone. Arrow: Left paracondylar tubercle. 1r/1l: right/left transverse process of C1. 2r/2l: right/left lateral mass of C1. 3r/3l: right/left occipital process. No presence of joint between the left paracondylar tubercle and the left transverse process of C1.



233
234
235
236
237
238
239
240
241
242
243
244
245
246
247

Fig. 5. Patient n°1. Planmeca Promax 3D Mid. Sagittal two-dimensional (2D) view. * Left paracondylar tubercle. LTP: left transverse process.

248

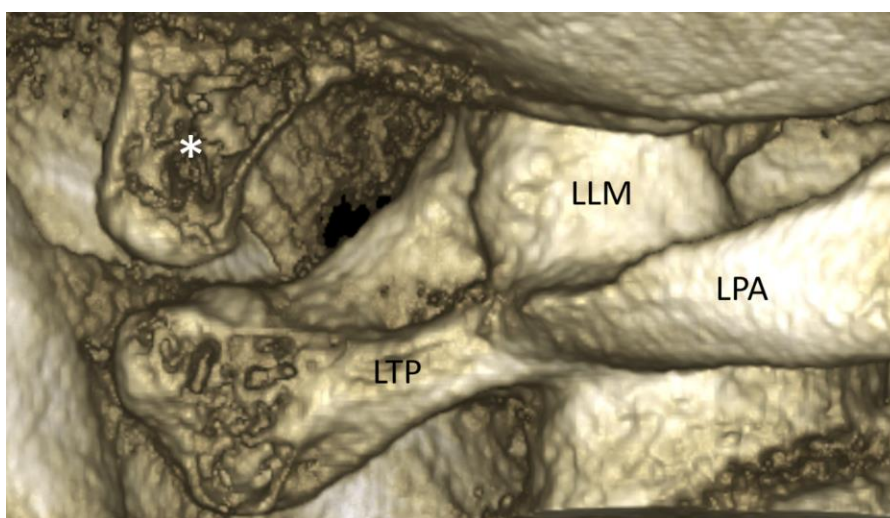
Unilateral paracondylar process with cylindrical shape

249

Fig. 6. Patient n°2. Planmeca Promax 3D Mid. 3D reconstruction. Posterior view. *Left paracondylar process. LLM: left lateral mass. RLM: right lateral mass. LPA: left posterior arch of C1. RPA: right posterior arch of C1. LTP: left transverse process of C1. RTP: right transverse process of C1. The superior edges of LTP and RTP are flat. There is no joint between the *Left paracondylar process and LTP.

255

256



257

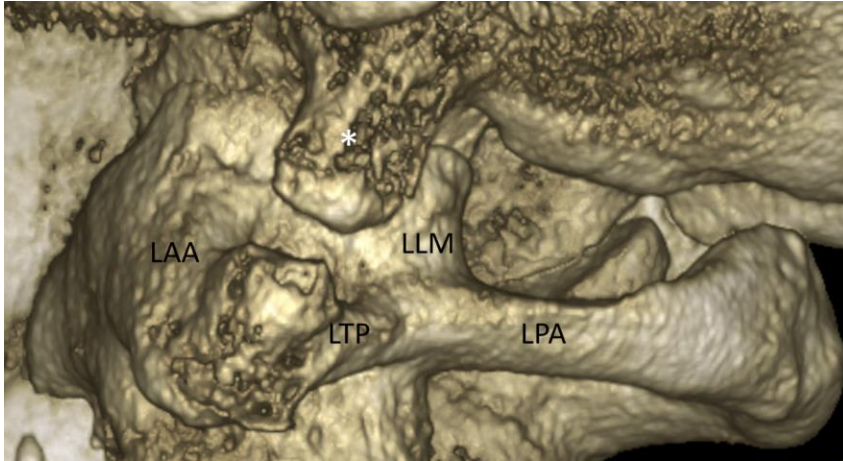
Fig. 7. Patient n°2. Planmeca Promax 3D Mid. 3D reconstruction. Closer posterior and left lateral view. *Left paracondylar process of cylindrical shape. LLM: left lateral mass. LPA: left posterior arch of C1. LTP: left transverse process.

261

262

263

264



265

266

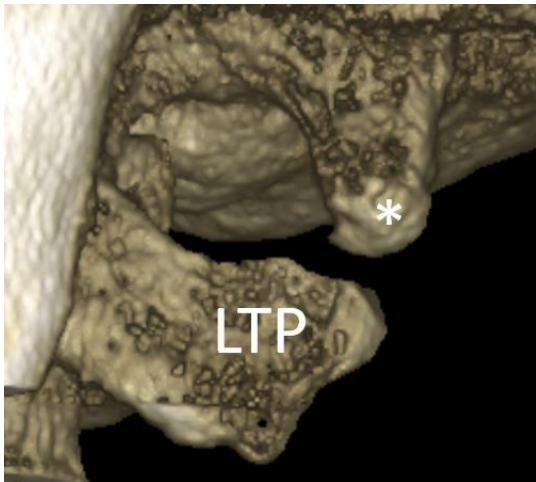
267

268

269

270

Fig. 8. Patient n°2. Planmeca Promax 3D Mid. 3D reconstruction. Left sagittal view. *Left paracondylar process of cylindrical shape. LLM: left lateral mass. LPA: left posterior arch of C1. LTP: left transverse process. LAA: left anterior arch of C1.



271

272

273

274

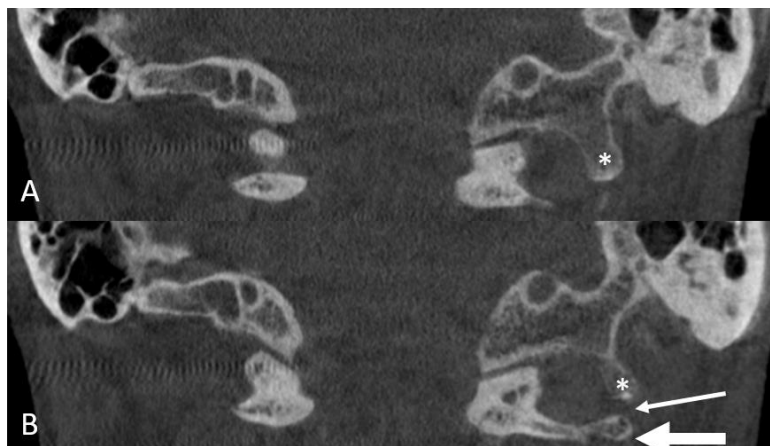
275

276

277

278

Fig. 9. Patient n°2. Planmeca Promax 3D Mid. 3D reconstruction. Left sagittal view. *Left paracondylar process of cylindrical shape. LTP: left transverse process. No joint between *Left paracondylar process and LTP.

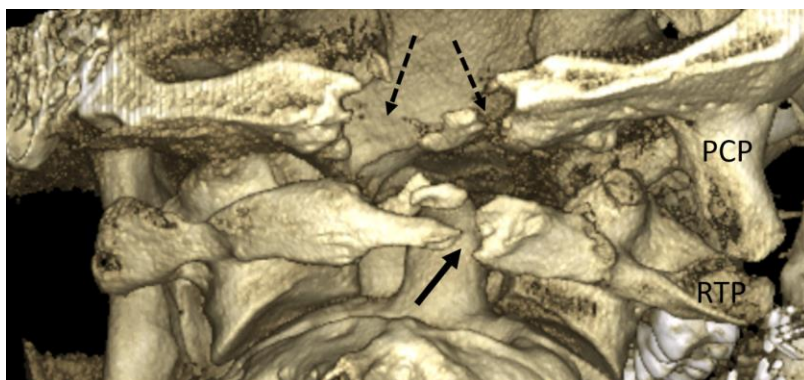


279

280 **Fig. 10.** Patient n°2. Planmeca Promax 3D Mid. Coronal two-dimensional
 281 (2D) view. A. More posterior view. *Left paracondylar process of cylindrical
 282 shape. B. More anterior view. *Left paracondylar process. Thick arrow: LTP.
 283 Thin arrow: distance between both structures.
 284

285

Unilateral paracondylar process with pyramidal shape



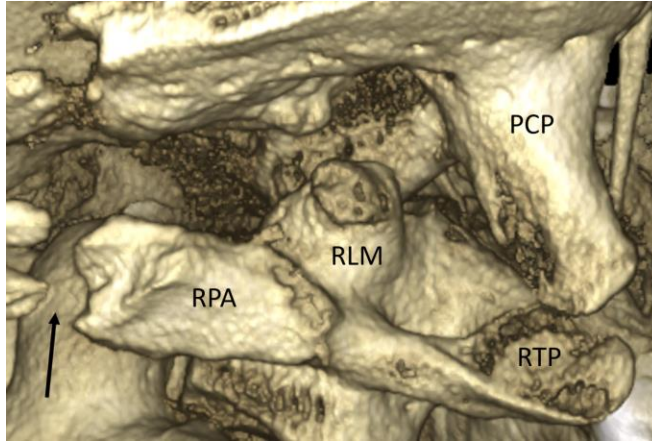
286

287 **Fig. 11.** Patient n°3. Planmeca Promax 3D Mid. 3D reconstruction. Posterior
 288 view. PCP: paracondylar process. RTP: right transverse process of C1.
 289 Black arrow: splitting of posterior arch and traces of sequestered bone
 290 (sequellae after cranial trepanation). Dashed arrows: traces of occipital bone
 291 trepanation.

292

293

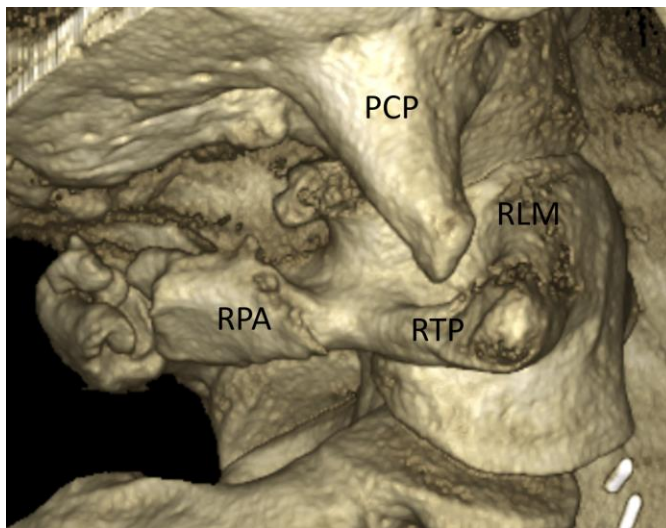
294



295

296 **Fig. 12.** Patient n°3. Planmeca Promax 3D Mid. 3D reconstruction. Posterior
297 view. PCP: paracondylar process. RLM: right lateral mass. RPA: right
298 posterior arch of C1. RTP: right transverse process (flat). Black arrow:
299 splitting of the posterior arch on the midline.

300



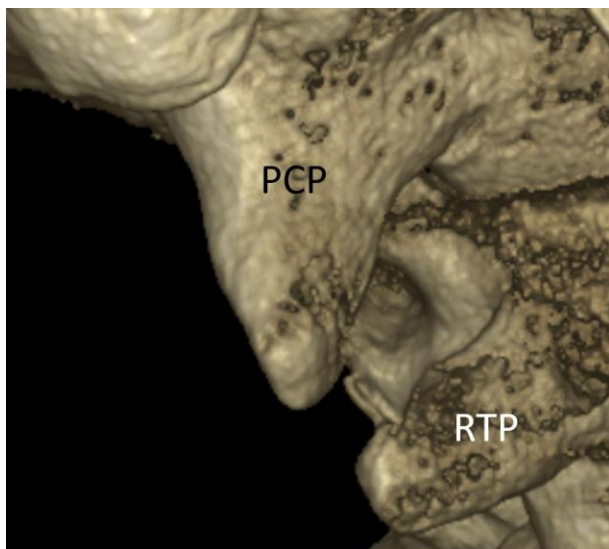
301

302 **Fig. 13.** Patient n°3. Planmeca Promax 3D Mid. 3D reconstruction. Right
303 sagittal view. PCP: paracondylar process with pyramidal shape. RLM: right
304 lateral mass. RPA: right posterior arch. RTP: right transverse process. No
305 presence of joint structure between PCP and RTP.

306

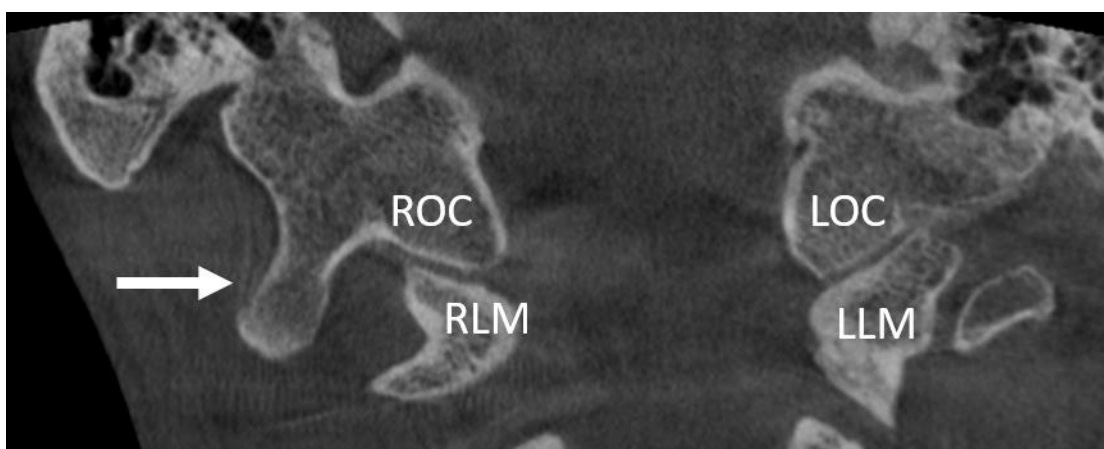
307

308



309
310
311
312
313

Fig. 14. Patient n°3. Planmeca Promax 3D Mid. 3D reconstruction. Right sagittal view. PCP: paracondylar process with pyramidal shape. RTP: right transverse process. Distance between both anatomic structures.



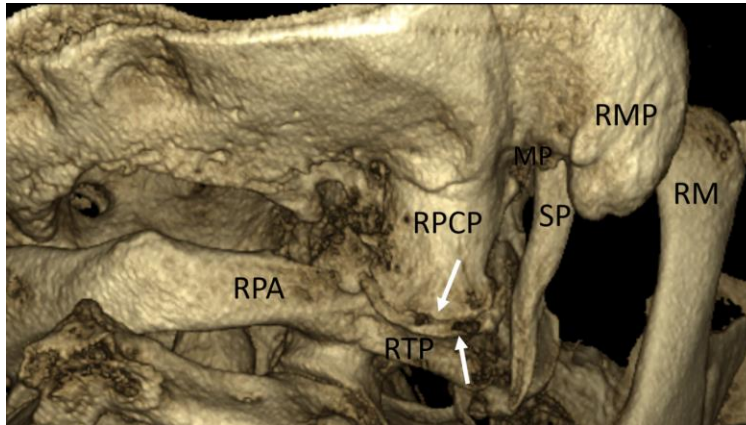
314

Fig. 15. Patient n°3. Planmeca Promax 3D Mid. Coronal 2D view. ROC: right occipital condyle. LOC: left occipital condyle. RLM: right lateral mass. LLM: left lateral mass. Arrow: right unilateral paracondylar process.

315
316
317
318
319
320
321
322

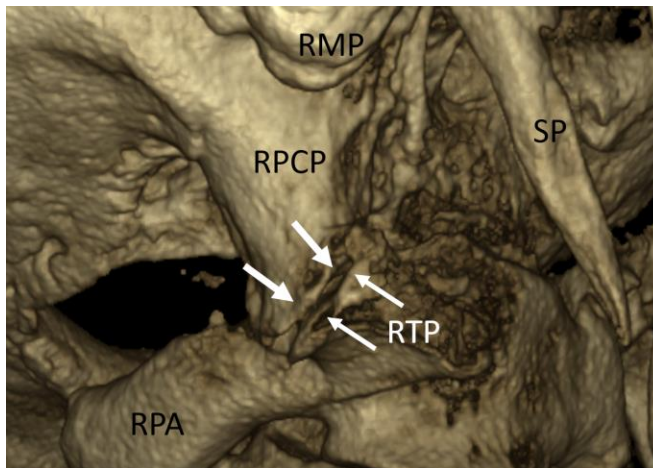
323
324

Unilateral paracondylar process with lateral joint with transverse process of C1



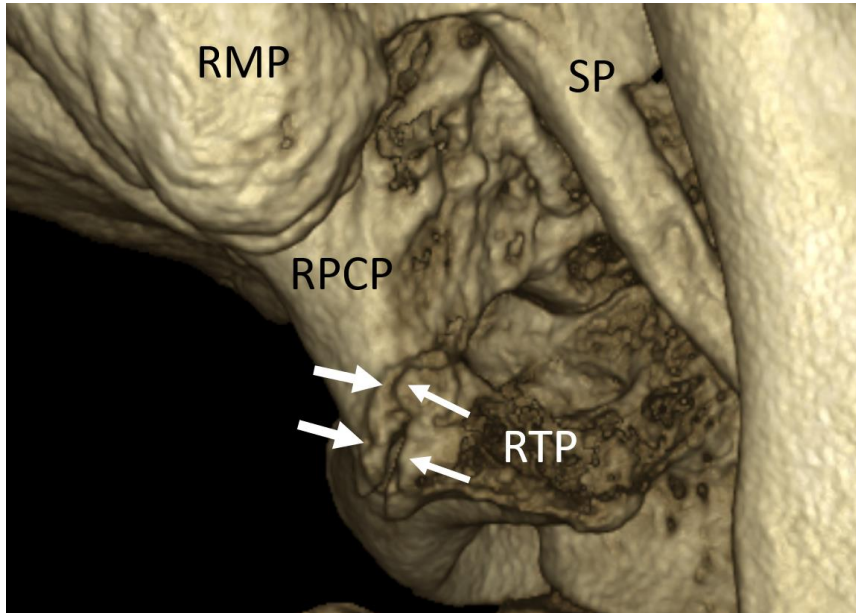
325

326 **Fig. 16.** Patient n°4. Planmeca Promax 3D Mid. 3D reconstruction. Posterior
327 view. RPCP: right paracondylar process. RTP: right transverse process.
328 RPA: right posterior arch of C1. SP: right styloid process. RMP: right mastoid
329 process. RM: right ramus of the mandible. White arrows: joint between
330 RPCP and RTP.
331



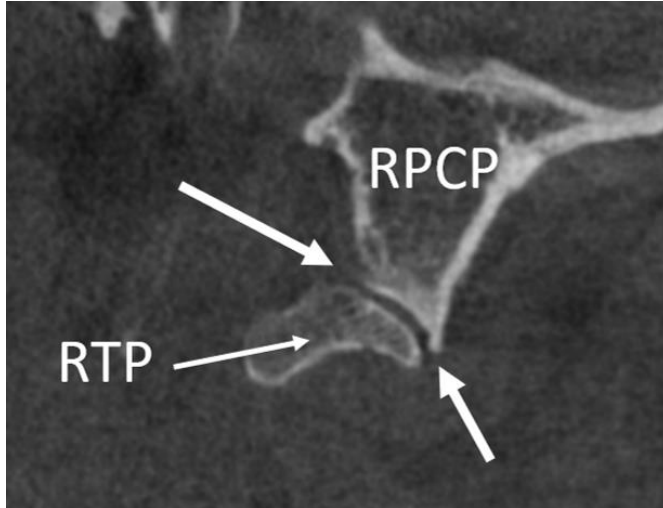
332

333 **Fig. 17.** Patient n°4. Planmeca Promax 3D Mid. 3D reconstruction. Right
334 lateral sagittal view. RPCP: right paracondylar process of pyramidal shape.
335 RTP: right transverse process. RPA: right posterior arch. RMP: right mastoid
336 process. SP: right styloid process. Arrows: lateral joint between RPCP and
337 RTP.



338

339 **Fig. 18.** Patient n°4. Planmeca Promax 3D Mid. 3D reconstruction. Right
340 sagittal view. RPCP: right paracondylar process. RTP: right transverse
341 process. RMP: right mastoid process. SP: right styloid process. Arrows:
342 lateral joint between RPCP and RTP.
343
344
345
346
347
348
349
350
351
352
353



354

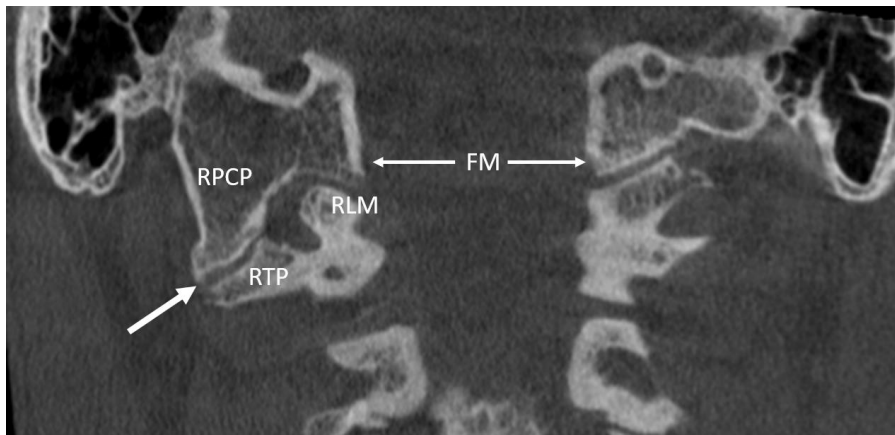
355

356

357

358

Fig. 19. Patient n°4. Planmeca Promax 3D Mid. Right sagittal 2D view. RPCP: right paracondylar process. RTP: right transverse process. Arrows: lateral joint between RPCP and RTP.



359

360

361

362

363

364

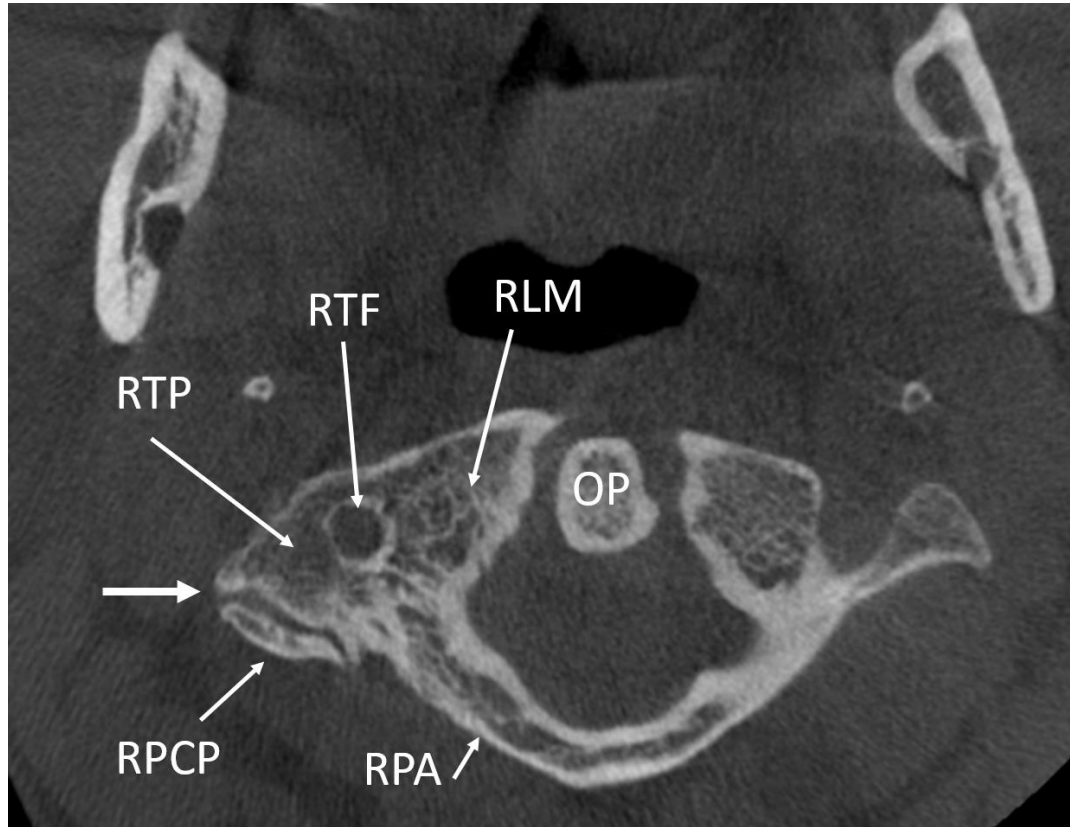
365

366

367

368

Fig. 20. Patient n°4. Planmeca Promax 3D Mid. Coronal 2D view. RPCP: right paracondylar process. RTP: right transverse process. RLM: right lateral mass. FM: foramen magnum. Arrows: lateral joint between RPCP and RTP.

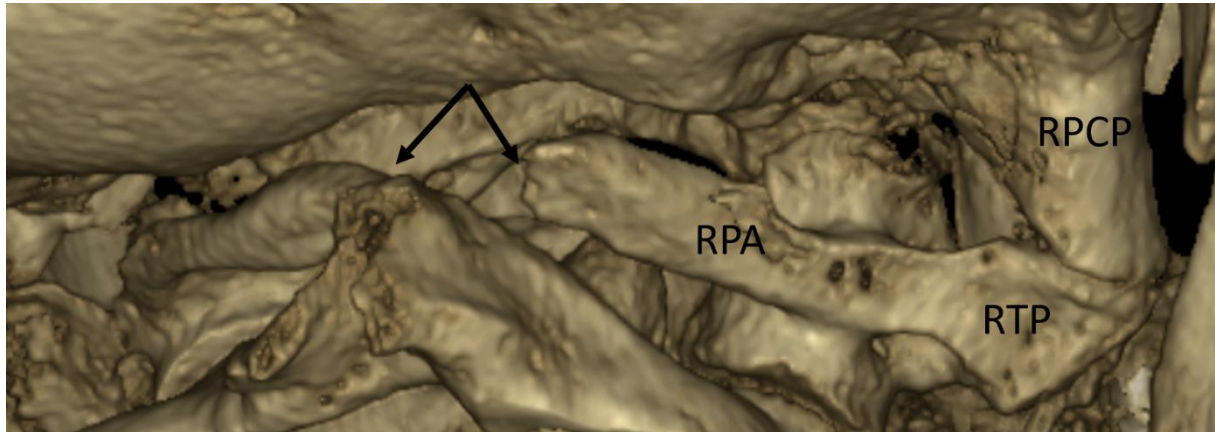


369
370
371 **Fig. 21.** Patient n°4. Planmeca Promax 3D Mid. Axial view. "Tropical fish"-
372 Clownfish image with "open mouth". RPCP: right paracondylar process.
373 RTP: right transverse process. RTF: right transverse foramen. RLM: right
374 lateral mass. RPA: right posterior arch. OP: odontoid process. Arrow: lateral
375 and posterior joint between RPCP and RTP.

375
376
377
378
379
380
381
382
383
384
385
386

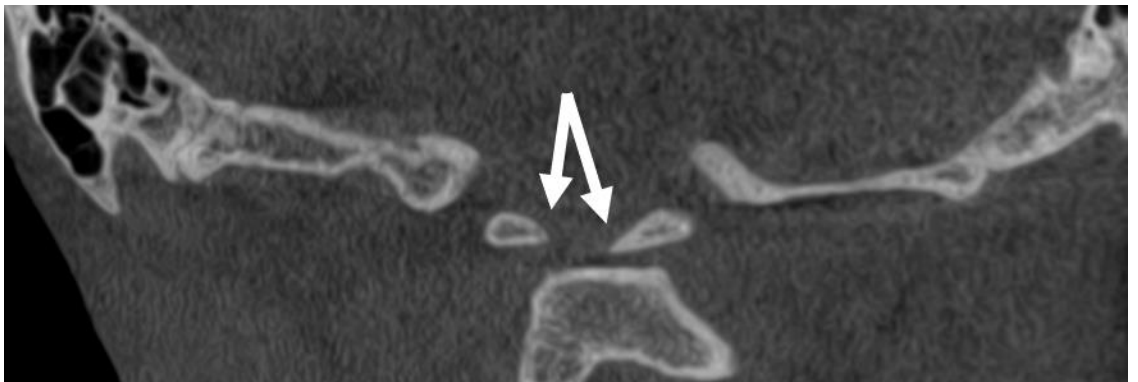
387
388

Unilateral paracondylar process with superior joint and partial fusion with transverse process of C1



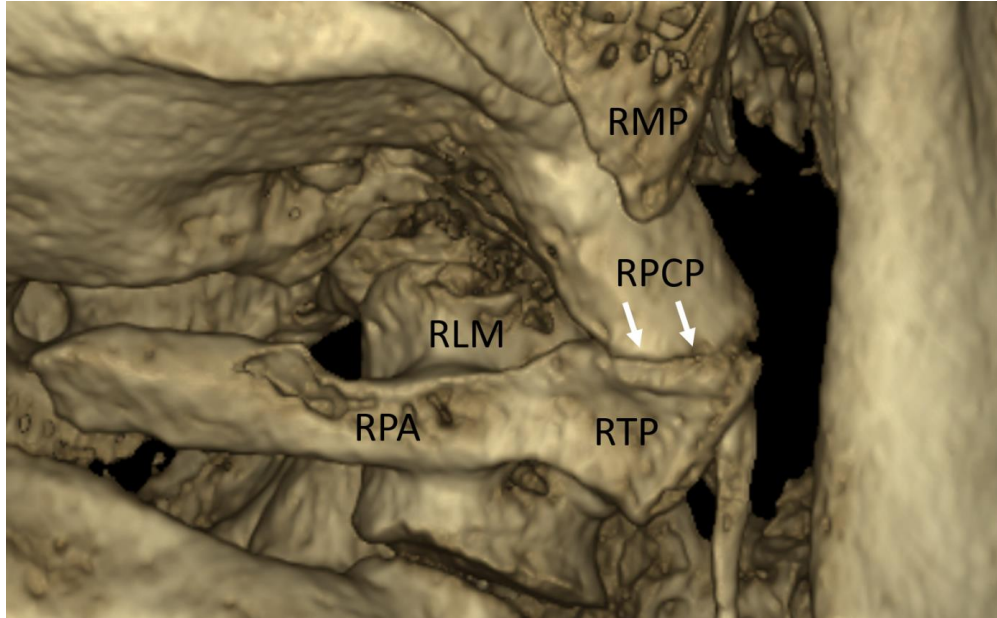
389

390 **Fig. 22.** Patient n°5. Planmeca Promax 3D Mid. 3D reconstruction. Posterior
391 view. RPCP: right paracondylar process. RTP: right transverse process.
392 RPA: right posterior arch. Black arrows: absence of fusion between posterior
393 arches of C1 on the midline.
394



395

396 **Fig. 23.** Patient n°5. Planmeca Promax 3D Mid. Coronal 2D view. Arrows:
397 absence of fusion between posterior arches of C1 on the midline.
398
399
400
401
402
403
404



405

406 **Fig. 24.** Patient n°5. Planmeca Promax 3D Mid. 3D reconstruction. Posterior
407 view. RPCP: right paracondylar process. RTP: right transverse process.
408 RPA: right posterior arch. RLM: right lateral mass. RMP: right mastoid
409 process. Arrows: joint between RPCP and RTP on the superior edge of the
410 RTP.

411

412

413

414

415

416

417

418

419

420

421

422

423

424

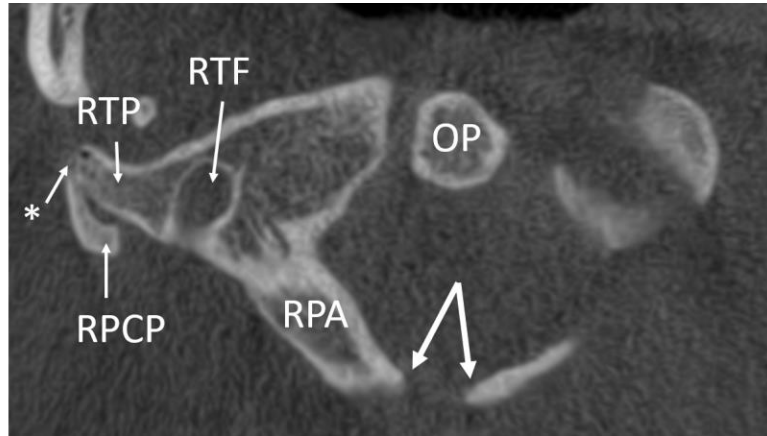
425

426

427

428

429

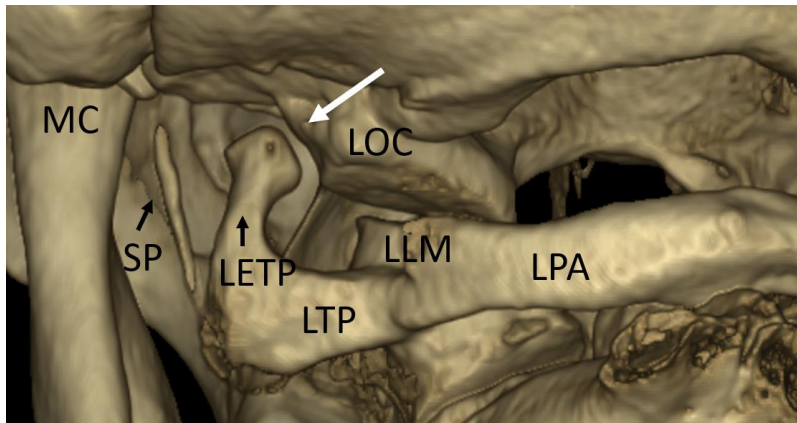


430
431
432
433
434
435
436

Fig. 25. Patient n°5. Planmeca Promax 3D Mid. 2D axial view. “Tropical fish Butterflyfish” image with “closed mouth”. RPCP: right paracondylar process. RTP: right transverse process. RPA: right posterior arch. RTF: right transverse foramen. OP: odontoid process. Joint between RPCP and RTP. * Fusion between lateral part of RPCP and RTP.

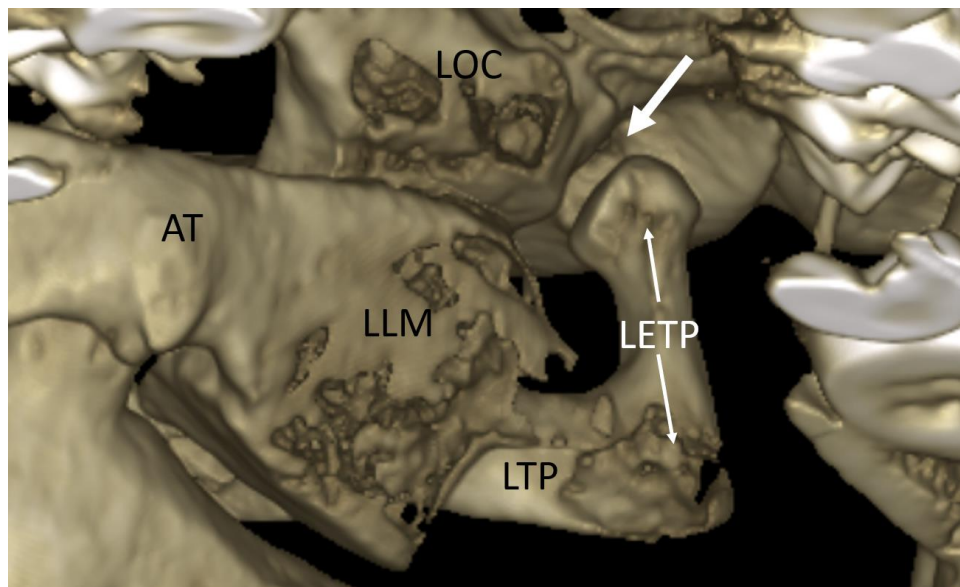
437
438

Unilateral epitransverse process with neo-condyle and joint with occipital condyle



439
440
441
442
443
444
445

Fig. 26. Patient n°6. Planmeca Promax 3D Mid. 3D reconstruction. Posterior view. LETP: left epitransverse process. LTP: left transverse process. LLM: left lateral mass. LPA: left posterior arch. LOC: left occipital condyle. SP: left styloid process. MC: left mandibular condyle. Arrow: neo-condyle at the summit of the LETP.



446

447

448

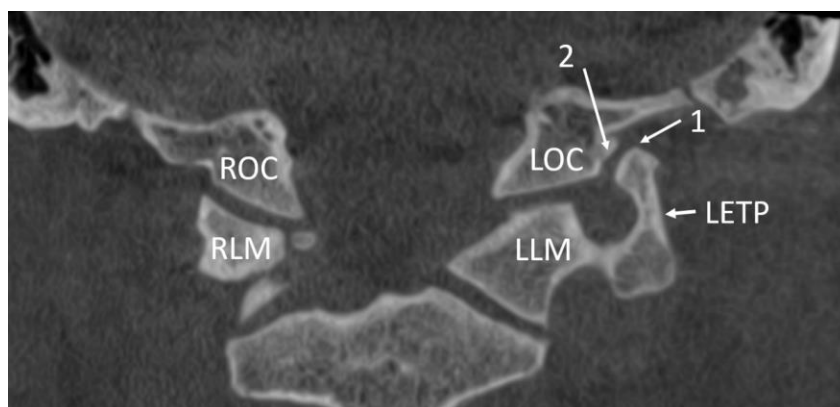
449

450

451

452

Fig. 27. Patient n°6. Planmeca Promax 3D Mid. 3D reconstruction. Anterior view of the left side. LETP: left epitransverse process. LTP: left transverse process. LLM: left lateral mass. LOC: left occipital condyle. AT: atlas tubercle. Arrow: neo-fossa on the lateral side of LOC in relationship with neo-condyle of LETP.



453

454

455

456

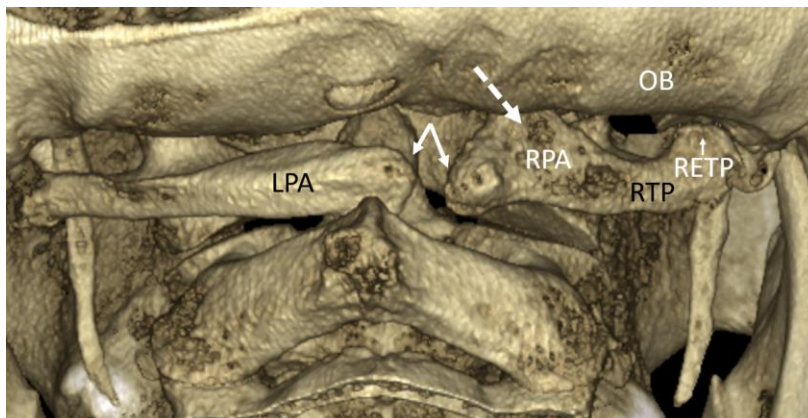
457

458

Fig. 28. Patient n°6. Planmeca Promax 3D Mid. Coronal 2D view. LETP: left epitransverse process. LTP: left transverse process. LLM: left lateral mass. LOC: left occipital condyle. ROC: right occipital condyle. RLM: right lateral mass. 1. Neo-condyle of LETP. 2. Neo-fossa on lateral side of LOC.

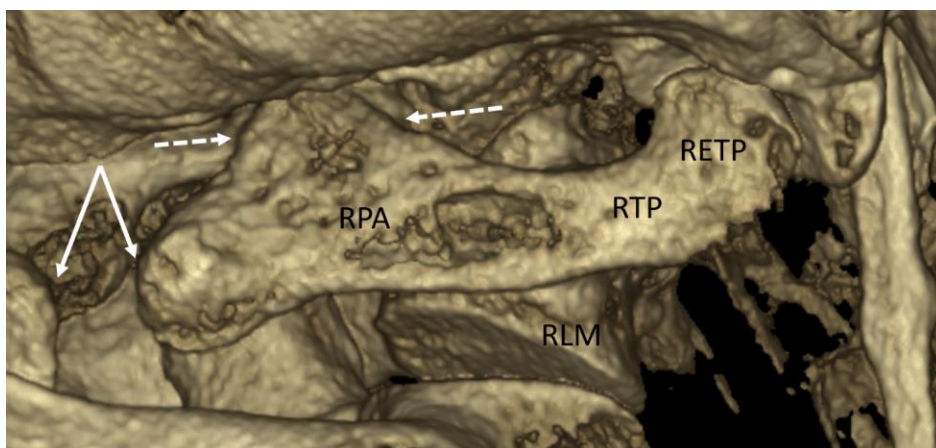
459
460

Unilateral epitransverse process with joint with occipital bone



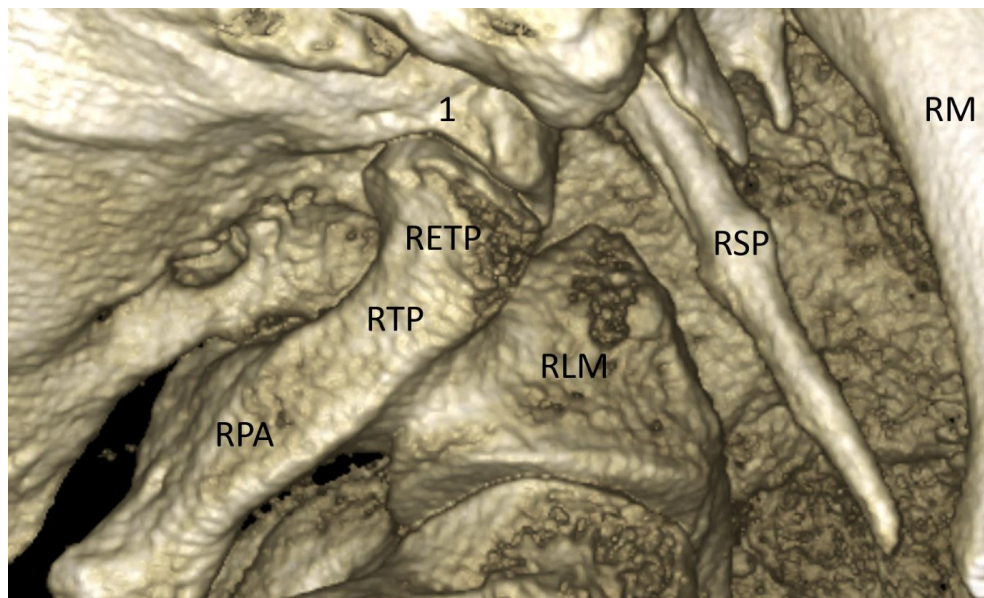
461

462 **Fig. 29.** Patient n°7. Planmeca Promax 3D Mid. 3D reconstruction. Posterior
463 view. RETP: right epitransverse process. RTP: right transverse process.
464 RPA: right posterior arch of C1. LPA: left posterior arch of C1. OB: occipital
465 bone. Dashed arrow: exostosis of the upper edge of the RPA (calcification of
466 posterior atlantooccipital membrane). Arrows: absence of fusion of posterior
467 arches of C1 on the midline. RETP in close relationship with OB.
468



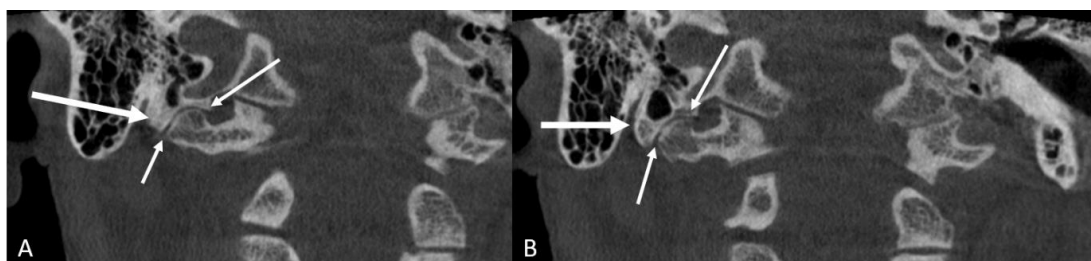
469

470 **Fig. 30.** Patient n°7. Planmeca Promax 3D Mid. 3D reconstruction. Posterior
471 view. RETP: right epitransverse process. RTP: right transverse process.
472 RPA: right posterior arch of C1. RLM: right lateral mass. Dashed arrows:
473 pyramidal exostosis of the upper edge of the RPA. Arrows: absence of
474 fusion of posterior arches of C1 on the midline.



475
476
477
478
479
480
481

Fig. 31. Patient n°7. Planmeca Promax 3D Mid. 3D reconstruction. Lateral and posterior view. RETP: right epitransverse process. RTP: right transverse process. RPA: right posterior arch of C1. RLM: right lateral mass. RSP: right styloid process. RM: right mandible. 1. Neo-fossa on the occipital bone corresponding to the summit of the RETP.



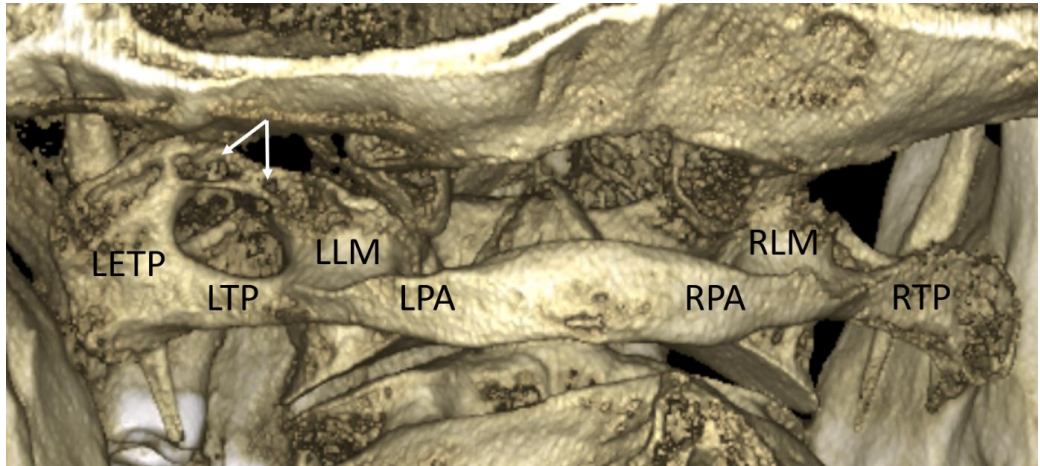
482

483
484
485
486
487
488
489
490
491

Fig. 32. Patient n°7. Planmeca Promax 3D Mid. A. Coronal 2D view. Thin arrows: joint between RETP and OB. Thick arrow: Neo-fossa belonging to OB in close relationship with RETP. B. Coronal 2D view. Thin arrows: joint between RETP and OB. Thick arrow: OB with pneumatization. Joint exists between OB and RETP.

492
493

Unilateral epitransverse process with a bony bridge with lateral mass (ponticulus lateralis)



494

495 **Fig. 33.** Patient n°8. Planmeca Promax 3D Mid. 3D reconstruction. Posterior
496 view. LETP: left epitransverse process. LTP: left transverse process. LPA:
497 left posterior arch of C1. LLM: left lateral mass. RTP: right transverse
498 process. RLM: right lateral mass. RPA: right posterior arch of C1. Arrows:
499 thick bony bridge between the summit of LETP and lateral and upper side of
500 LLM (ponticulus lateralis).

501

502

503

504

505

506

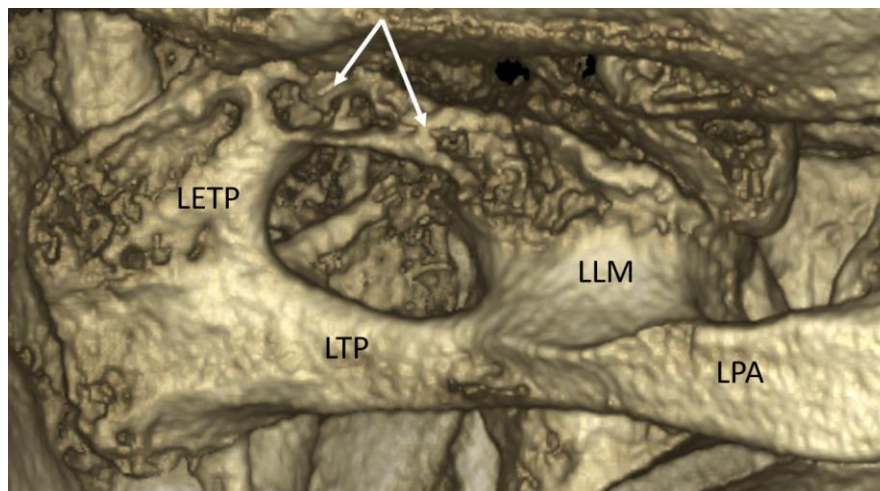
507

508

509

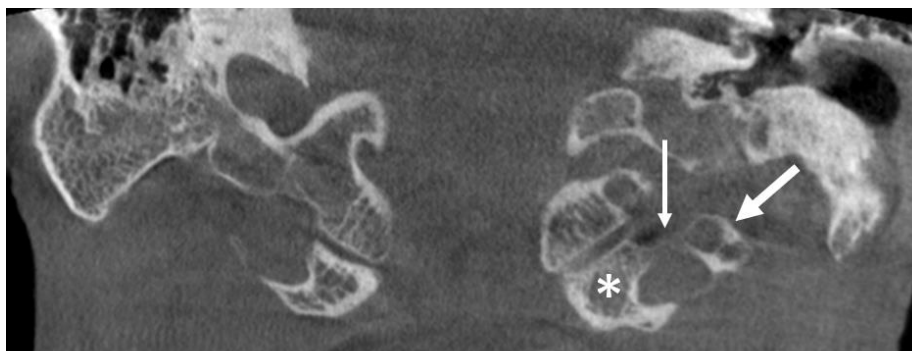
510

511



512

513 **Fig. 34.** Patient n°8. Planmeca Promax 3D Mid. 3D reconstruction. Posterior
514 view. Zoom on the LETP variation. Posterior view. LETP: left epitransverse
515 process. LTP: left transverse process. LPA: left posterior arch of C1. LLM:
516 left lateral mass. Arrows: thick bony bridge between LETP and LLM
517 (ponticulus lateralis), and without occipitalisation.
518

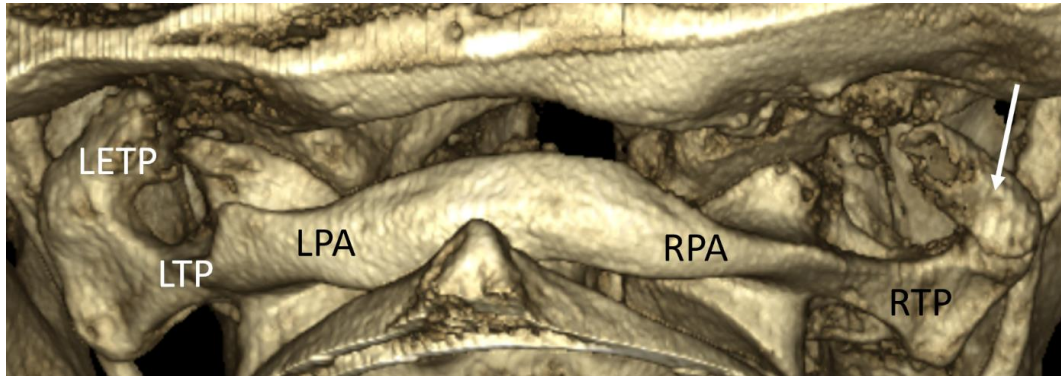


519

520 **Fig. 35.** Patient n°8. Planmeca Promax 3D Mid. Coronal 2D view. *LLM.
521 Thick arrow: LETP. Thin arrow: bony bridge between both structures
522 (ponticulus lateralis). There is still space between the bony bridge and the
523 occipital bone.
524
525
526
527
528
529

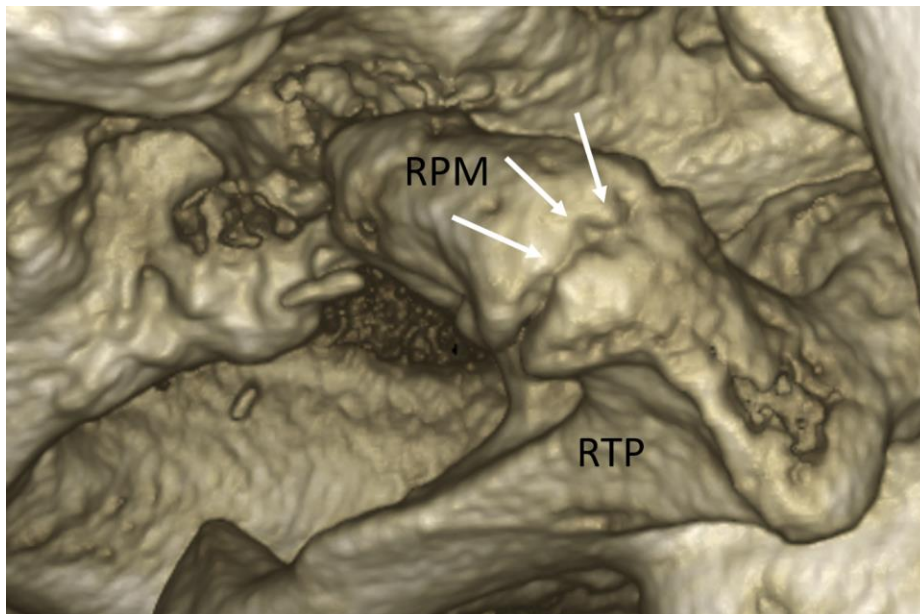
530
531

Bilateral variation: paracondylar mass and epitransverse process



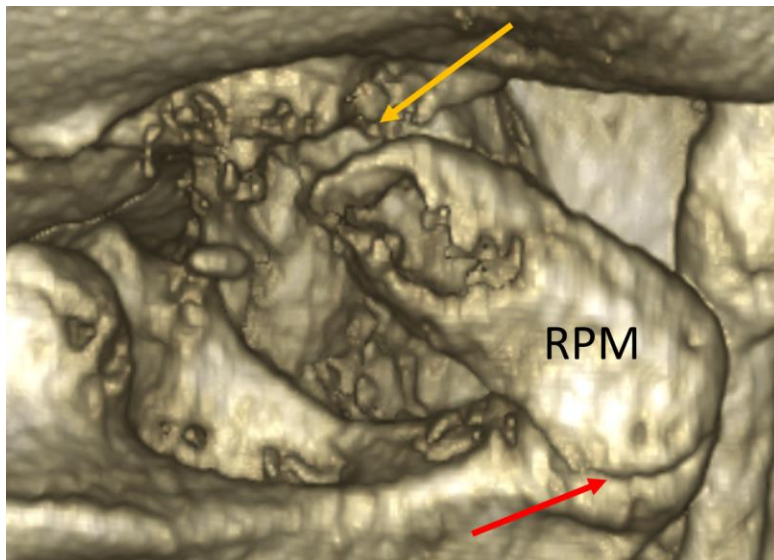
532
533
534
535
536
537
538

Fig. 36. Patient n°9. Planmeca Promax 3D Mid. 3D reconstruction. Posterior view. LETP: left epitransverse process. LTP: left transverse process. LPA: left posterior arch of C1. RPA: right posterior arch of C1. RTP: right transverse process. Arrow: paracondylar mass between RTP (joint) and the occipital bone.



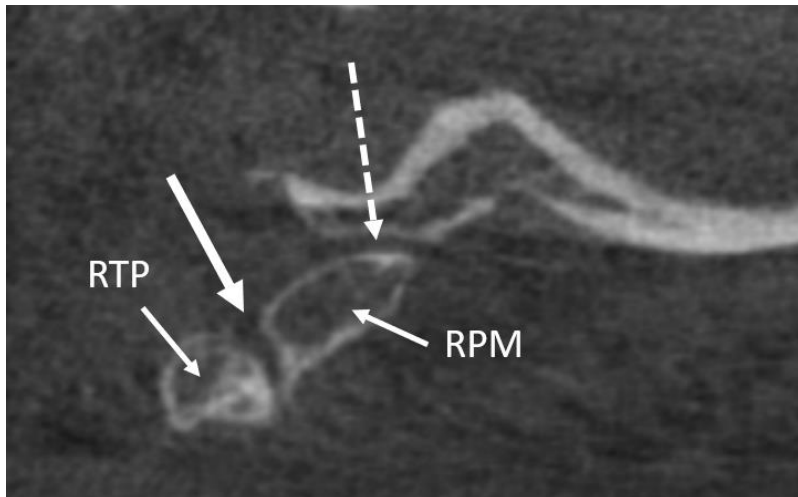
539
540
541
542

Fig. 37. Patient n°9. Planmeca Promax 3D Mid. 3D reconstruction. Posterior view centred on right paracondylar mass (RPM). RTP: right transverse process. Arrows: joint between RPM and the upper area of RTP.



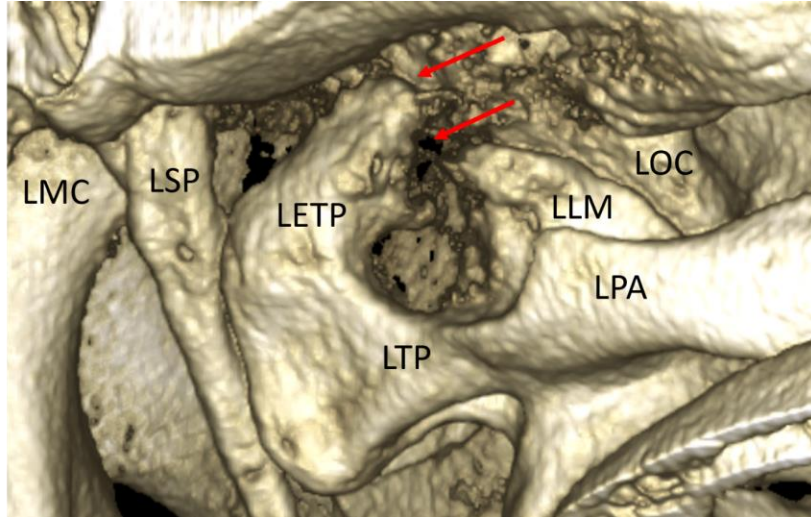
543
544
545
546
547
548

Fig. 38. Patient n°9. Planmeca Promax 3D Mid. 3D reconstruction. Posterior view centred on right paracondylar mass (RPM). Red arrow: joint between RPM and the upper area of RTP. Orange arrow: distance between the summit of RPM and the occipital bone, without any joint.



549
550
551
552
553
554

Fig. 39. Patient n°9. Planmeca Promax 3D Mid. Sagittal 2D view. RPM: right paracondylar mass. RTP: right transverse process. Thick arrow: joint between RPM and RTP on the posterolateral side of RTP. Dashed arrow: no joint between RPM and occipital bone.



555

556 **Fig. 40.** Patient n°9. Planmeca Promax 3D Mid. 3D reconstruction. Posterior
557 view. LETP: left epitransverse process. LTP: left transverse process. LPA:
558 left posterior arch of C1. LLM: left lateral mass. LOC: left occipital condyle.
559 LSP: left styloid process. LMC: left mandibular condyle. Red arrows: LETP
560 without joint with LLM or with occipital bone.
561



562 **Fig. 41.** Patient n°9. Planmeca Promax 3D Mid. Coronal 2D view. *Right
563 paracondylar mass without joint with the occipital bone. **left epitransverse
564 process without joint with the occipital bone.
565
566
567
568
569

570

Discussion

571

572

573

574

575

576

577

578

579

580

581

582

583

584

585

586

587

588

589

590

591

592

The selected literature provided us only with case reports of single patients [3-7]. We were able to present the first clinical series of 9 patients with PCP/ETP variations. Only a CT scan was used in previously reported cases. In our series we exclusively used a CBCT (Planmeca Promax 3D mid).

Bertini et al. [7], proposed in 1991 a classification of variations of PCP and of ETP with 7 different types described on coronal view (Table 1). Bertini's classification was based on previous studies and classifications by Zimmer in 1973 [8], and by Wackenheim in 1983 [9]. Bertini's classification was limited to unilateral variations. We completed this classification by adding: 1) Bilateral variations (identical or different on right/left side), 2) Joint existing between PCP and ETP (called by the author "dugong head image" [4]), 3) Joint of ETP with the lateral side of occipital condyle, 4) Presence of bony bridge (ponticulus lateralis) between ETP and the lateral mass of C1. We also found a variation in the shape of PCP: cylindrical and pyramidal. Only pyramidal (triangular) shape was already described [5, 7].

In Bertini's classification we can find the expression "C1 lateral mass" in relation with PCP. However, the figures and drawings from Bertini's article show that PCP is in anatomical relationship with the transverse process of C1 and not with the lateral mass [7]. Therefore, we replaced the term "C1 lateral mass" by "C1 transverse process" in the definition of a given variation related with PCP.

Table 1. Classification of variations of paracondylar process and epitransverse process.

	Unilateral [7]	Bilateral (identical) [added by author]	Bilateral (mixt) [added by author]
Paracondylar tubercle: small bony prominence on the inferior margin of the occiput [7]	Figs. 1-5 (this study)		
Paracondylar process: a larger bony prominence which originates next to the occipital condyle and projects caudally toward the C1 lateral mass [7] (<i>not on C1 lateral mass but on C1 transverse process</i>)	Fig. 2, CT scan, pyramidal shape [5] Figs. 6-25 (this study) Figs. 6-10: cylindrical shape (this study) Figs. 11-25: pyramidal shape (this study)		
Joint between paracondylar process and the lateral mass of C1 (<i>not on C1 lateral mass but on C1</i>)	Fig. 1A, fig. 1C, CT scan [6] Fig. 2, CT scan, coronal view [7] Figs. 16-25 (this study)		

<i>transverse process</i>) [7]	Fig. 21, "Tropical Clownfish" image (this study), Fig. 25, "Tropical Butterflyfish" image (this study)		
Joint between paracondylar process with epitransverse process [added by author]	Fig. 2, and Fig. 2B, CT scan, "dugong head" image [4] (author's denomination)		
Fusion of paracondylar process with C1 lateral mass (<i>not on C1 lateral mass but on C1 transverse process</i>) [7]	Fig. 25, "Tropical butterflyfish" image, (this study)		
Paracondylar mass (or <i>massa paracondylarica</i> [5]): an isolated bony mass located between occiput and C1 transverse process [7]	https://radiopaedia.org/articles/paracondylar-process?lang=us CT scan, case n°2		Figs. 36-39, 41 (this study)
Epitranverse process [7]	https://radiopaedia.org/articles/epitranverse-process-of-the-atlas CT scan, case n°2 Fig. 1, CT scan, [3] Fig. 2, CT scan, [4] Figs. 26-41 (this study)		Figs. 36, 40, 41 (this study)
Joint between epitranverse process and lateral side of occipital condyle [added by the author]	Figs. 26-28 (this study)		
Joint between epitranverse process and a bony prominence of the occiput [7]	https://radiopaedia.org/articles/epitranverse-process-of-the-atlas CT scan, case n°2 Figs. 29-32 (this study)		
Presence of bony bridge between epitranverse process and lateral mass of C1 [added by the author]	Figs. 33-35 (this study)		

594 Six figures were found in the selected literature [3-7], and belonged only to
595 articles published in closed access (payment or subscription needed to access the
596 article). Two volumes of CT scan images (one case of unilateral PCP and one case
597 of unilateral ETP) were freely available on radiopaedia.org. We provided with addi-
598 tional 41 open access freely available figures. Table 1 presents 30 variations of PCP
599 and ETP instead of initial 7 variations presented in Bertini's article [7].
600 Only 12 of 30 possible variations were described in this study with 6 variations
601 already described previously, and 6 new variations added by this study.
602 We were first to present with CBCT figures of the following: 1) unilateral
603 paracondylar tubercle, 2) a fusion of PCP with the transverse process of C1, 3) a
604 joint between ETP and the lateral side of the occipital condyle, and 4) the presence
605 of bony bridge (ponticulus lateralis) between the ETP and the lateral mass of C1.
606 We were also first to describe a bilateral mixt variation with paracondylar mass on
607 one side and with the ETP on the other side of C1.
608 Bilateral cases from the literature are missing in our study due to the application of
609 our exclusion criteria. For example, Narayanan et al, published an open access
610 article on a single case of bilateral PCP with articulation on transverse process (3
611 figures, CT scan) [10]. However, Narayanan's article was published without abstract
612 [10]. Moreover, the existence of bilateral mixt cases (each side with a different
613 variation) opens much broader perspective on diversity of possible associations and
614 of types of joints existing between structures that may be present in humans.
615 We introduced also three "radiological animal signs" images [11]. Radiological
616 animal signs images are widely used in radiological education [11, 12].
617 Joint between the PCP and the transverse process of C1, and with or without fusion
618 were compared on axial view to "tropical Butterflyfish" with a closed mouth (Fig.
619 25) or a "tropical Clownfish" with an open mouth (Fig. 21). The joint between the
620 PCP and the ETP looked like the "dugong head" in McCall et al., [4] (Figure 2B,
621 axial view, CT scan).
622 In two of nine patients we found the congenital absence of fusion of posterior arch
623 on the midline (patient n°5, figs. 22, 23, 25; and n°7, figs. 29, 30) We also found the
624 exostosis on the cranial edge of the right posterior arch of C1 (patient n°7, figs. 29,
625 30) which may correspond to the calcification of the posterior atlanto-occipital
626 membrane. However, as our patients series is too small we cannot conclude on any
627 association between those findings and the presence of PCP and/or ETP.
628 As we are responsible of the full field of view, and when using large field of view of
629 CBCT (16cm of diameter) we may find rare anatomical variations related to the
630 skull base and to the cervical vertebra. An open and accessible knowledge support
631 (such as Nemesis or other future journals) is then needed to easily find clinical
632 reference figures described and provided by specialists in dentomaxillofacial
633 radiology.

634

635

636

637

- **Acknowledgements:** none

638

- **Funding sources statement:** this study does not receive any funding.

639

- **Competing interests:** Prof R. Olszewski is the Editor-in-Chief of Nemesis.

640

- **Ethical approval:** We obtained the approval from our University and Hospital Ethical committee for this study (B403/2019/03DEC/542)

641

642

- **Informed consent:** Patients were exempted from the informed consent according to the ethical committee approval.

643

644

Authors contribution:

Author	Contributor role
Olszewski Raphael	Conceptualization, Investigation, Methodology, Data curation, Resources, Validation, Writing original draft preparation, Supervision, Writing review and editing

645

646

References

647

1. Schumacher M, Yilmaz E, Iwanaga J, Oskouian R, Tubbs RS. Paramastoid process: Literature review of its anatomy and clinical implications. World Neurosurg 2018ep;117:261-263. doi: 10.1016/j.wneu.2018.06.056.

648

649

650

651

2. Mcrae DL. The significance of abnormalities of the cervical spine: Caldwell lecture, 1959. Am J Roentgenol 1960;84:3-25.

652

653

654

3. Isidro A, Burdeus JM, Loscos S, Bara J, Bosch J, Gallart A. Surgical treatment for an uncommon headache: A gap of 4800 years. Cephalalgia 2017;37:1098-1101. doi: 10.1177/0333102416665227.

655

656

657

658

4. McCall T, Coppens J, Couldwell W, Dailey A. Symptomatic occipitocervical paracondylar process. J Neurosurg Spine 2010;12:9-12. doi: 10.3171/2009.7.SPINE09345.

659

660

661

662

5. de Graauw N, Carpay HA, Slooff WB. The paracondylar process: an unusual and treatable cause of posttraumatic headache. Spine (Phila Pa 1976) 2008;33:E283-E286. doi: 10.1097/BRS.0b013e31816d8d68.

663

664

- 665
666 6. Shah MJ, Kaminsky J, Vougioukas VI. Surgical removal of a symptomatic
667 paracondylar process. *J Neurosurg Spine* 2009;10:474-475. doi:
668 10.3171/2009.2.SPINE08461.
669
- 670 7. Bertini G, Celenza M, Orsi R, Porrati PL, Rolandi G. Osseous anomalies of the
671 craniovertebral junction: a case report. *Ital J Orthop Traumatol* 1991;17:135-139.
672
- 673 8. Zimmer EA. Piccole varietà ed anomalie delle prime vertebre cervicali.
674 *Radiologia Medica* 1973;59:673-688.
675
- 676 9. Wackenheim A. Radiodiagnosis of the vertebrae in adults. Springer-Verlag.
677 Berlin, Heidelberg, New York, 1983
678
- 679 10. Narayanan R, Shankar B, Paruthikunnan SM, Kulkarni CD. Paracondylar
680 process of the occipital bone of the skull: a rare congenital anatomical variant. *BMJ*
681 *Case Rep* 2014;2014:bcr2014205315. doi: 10.1136/bcr-2014-205315.
682
- 683 11. Ridley LJ. The use of animal signs in Radiology: Lessons in image interpretation
684 from art theory, patternicity and analogy. *J Med Imaging Radiat Oncol* 2018;62:3-6.
685 doi: 10.1111/1754-9485.12782
686
- 687 12. Foye P, Abdelshahed D, Patel S. Musculoskeletal pareidolia in medical
688 education. *Clin Teach* 2014;11:251-253.
689